

Research on the Performance and Diffusion Behavior of Geopolymer Grouting Material Made from Coal Roof Bottom Ash

Xinxin Yu*, Haibo Zhang, Yu Liu, Fengshun Zhang

School of Materials Science and Engineering, Henan Polytechnic University, Jiaozuo 454003, China

*Corresponding author: Xinxin Yu, yxyyds68@163.com

Copyright: © 2025 Author(s). This is an open-access article distributed under the terms of the Creative Commons Attribution License (CC BY 4.0), permitting distribution and reproduction in any medium, provided the original work is cited.

Abstract: As the cost of grouting treatment for water control in coal roofs during underground coal mining continues to rise, coupled with the accumulation of industrial solid waste resulting from rapid economic development in China, the ecological environment is facing severe challenges. To address these issues, this study, based on a high water-to-cement ratio, uses mine overburden (OB) and furnace bottom ash (FBA) as the primary raw materials, with sodium silicate as the modifier, to develop a new type of geopolymer grouting material with high stability and compressive strength for coal roof water control. Additionally, COMSOL software was used to numerically simulate the diffusion process of the grout slurry in fractures under dynamic water flow. The results indicate that, with a sodium silicate modulus of 1.5 and a dosage of 4%, the stability of the slurry increased by 26.2%, and the 28-day compressive strength improved by 130.98%. Numerical simulations further show that the diffusion process of the slurry is closely related to slurry viscosity, grouting pressure, and grouting time and that the diffusion pattern in the fractures is similar to that of ultra-fine cement slurry. This study provides a theoretical basis for coal mine roof grouting water control projects.

Keywords: Coal mine top grouting; Regional management; Numerical simulation; Comprehensive utilization; Solid waste

Online publication: February 10, 2025

1. Introduction

In underground engineering and mining, fissure water entering the excavation zone through rock pores and faults presents significant safety hazards. With the increase in excavation depth, water leakage from the coal seam roof not only corrodes equipment but also potentially causes harm to personnel^[1-3]. Ground grouting technology (as shown in **Figure 1**) has become a critical method for controlling water leakage from the coal seam roof^[4,5]. The performance of grouting materials directly impacts the quality of the grouting effect and the longevity of the project. Currently, there is a wide variety of grouting materials for the coal seam roof, with traditional materials such as cement grout and chemical grouts having good slurry properties, but they are expensive and have significant environmental impacts^[6-8]. According to incomplete statistics, the cement used in grouting releases

approximately 4×10^4 tons of carbon dioxide (CO_2) annually^[9]. Therefore, reducing the demand for cement in grouting material production and using solid waste to replace cement in large quantities is of great significance for achieving the “peak carbon emissions by 2023, carbon neutrality by 2060” goals^[10,11].

Currently, solid waste grouting materials mainly include slag, fly ash, or combinations of both. Yang et al. studied the properties of composite grouting materials based on cement, fly ash, and slag^[12]. Wang et al. developed a mortar using blast furnace slag for roadbed reinforcement, aiming to optimize the material’s rheological properties and mechanical strength^[13]. Li et al. explored the application of new calcium-based activators in coal bottom ash-based cementitious materials through orthogonal tests and range analysis^[14]. Bakhrakh et al. used coal ash and furnace slag as cement additives to increase the calcium, silicate, hydrate (C-S-H) gel content and the cement’s hydration degree^[15]. Fernandez et al. pointed out that the activity of fly ash is influenced by its silica and alumina content, exhibiting high late strength in geopolymers^[16].

However, existing research mostly focuses on improving a single property of the grout slurry under low water-to-cement ratios. However, applying solid waste in grouting water control requires a comprehensive evaluation of multiple properties of the slurry, including fluidity, stability, and compressive strength. Furthermore, the feasibility of using new materials in practical applications should be further investigated.

Mine overburden (OB) is the waste generated during coal mining, mainly consisting of useless minerals and rock fragments^[17]. Furnace bottom ash (FBA), a common industrial by-product, contains a certain amount of silicate and aluminate components^[18]. Incorporating OB into furnace bottom ash geopolymer not only facilitates the resource utilization of mine waste, reducing its environmental pollution and accumulation pressure but also provides new raw materials for construction^[19,20].

Based on the aforementioned background, this study, after extensive preliminary experiments, selected FBA, desulfurization gypsum (DSG), ordinary portland cement (OPC), and OB as the base materials. The research, under the premise of a high water-to-cement ratio, aims to improve the stability and compressive strength of the slurry and to develop a new type of grouting material with high stability and strength using solid waste resources. Finally, the diffusion characteristics of the new grouting material were simulated and evaluated using COMSOL numerical simulation software, providing a reference for the practical application of geopolymer grouting materials in coal mine roofs.

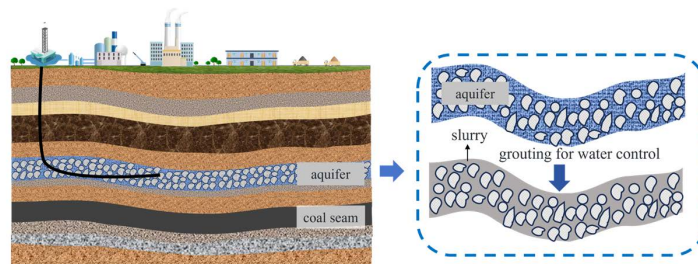


Figure 1. Schematic diagram of water control in the ground area

2. Experiment

2.1. Experimental materials

The FBA, DSG, and OPC used in the experiment were provided by Jiaozuo Qianye Cement Co., Ltd. The chemical composition of the main raw materials, FBA and OB, is shown in **Table 1**. OB was sourced from a mining area in Jiulishan, Jiaozuo City, naturally air-dried in its original state, and then ball-milled, with a specific surface area of $3261 \text{ m}^2/\text{kg}$. The calcium carbonate (CaCO_3) in OB mainly exists in the form of a calcite mineral structure, which exhibits water absorption, water retention, and slight expansion properties. These characteristics

help reduce the shrinkage of the stone body and improve overall moisture retention ^[21].

Table 1. Chemical composition of FBA and OB (%)

Component	CaO	SiO ₂	Al ₂ O ₃	MgO	Fe ₂ O ₃	K ₂ O	P ₂ O ₅	Burning loss
FBA	12.24	48.30	21.54	0.87	4.76	2.44	0.12	1.41
OB	46.18	28.16	10.72	7.85	3.56	2.58	0.52	5.36

Note: calcium oxide (CaO), silicon dioxide (SiO₂), aluminum oxide (Al₂O₃), magnesium oxide (MgO), iron oxide (Fe₂O₃), potassium oxide (K₂O), potassium pentoxide (P₂O₅)

2.2. Test and method

2.2.1. Experimental plan

Different amounts of sodium hydroxide (NaOH) solid were added to the sodium silicate solution to prepare sodium silicate with varying moduli. Through extensive preliminary experiments, it was determined that the geopolymer base was FBA: DSG: OPC: OB in a ratio of 45:2:3:50. For the stability test, a water-to-cement ratio of 1.8 was used, with sodium silicate of different moduli (1.3, 1.5, 2.4, 3.2) and addition amounts (2%, 4%, 6%, 8%) incorporated. For the geopolymer grouting material, the compressive strength test was conducted with a water-to-cement ratio of 0.4, and the curing age was set to 28 days. Three parallel samples were prepared for each group to minimize experimental errors. The specific experimental plan is shown in **Table 2**.

Table 2. Test scheme

Level	Modulus	Percentage (%)
1		2
2		4
3	1.3	6
4		8
5		2
6		4
7	1.5	6
8		8
9		2
10		4
11	2.4	6
12		8
13		2
14		4
15	3.2	6
16		8

2.2.2. Testing methods

- (1) Fluidity: The fluidity of the slurry was tested according to the Marsh funnel viscosity test method (SY/T 6864-2020, China).
- (2) Determination of water precipitation rate: The test was conducted according to the calculation method for

the water separation rate of concrete admixtures (GB 8076-2008, China).

- (3) Compressive strength: The compressive strength of the test specimens at 3 d, 7 d, and 28 d curing ages was tested according to the Cement Mortar Strength standard (GB/T17671-199, China) using a WHY-300/10 microcomputer-controlled pressure testing machine with a loading rate of 100 N/s.
- (4) X-ray diffraction (XRD): X-ray diffraction analysis was performed using a Smart X X-ray diffractometer (Japan). The testing conditions were set to 45 kV voltage, 200 mA current, a scanning speed of 10°/min, and a scanning range of 5° to 70°.
- (5) Scanning electron microscopy (SEM): The morphology of the hydration products was observed using a scanning electron microscope (SEM) from Zeiss (Germany), model Merlin Compact. The test specimens were cut and gold-coated before the SEM analysis.

3. Analysis of test results

3.1. Fluidity

The flowability of the geopolymer slurry under different modulus and dosages of sodium silicate shows varying trends, as illustrated in **Figure 2**. The flowability increases with the increase in the modulus of sodium silicate. This is primarily due to the higher sodium silicate modulus, which leads to a relatively higher content of sodium (Na^+) ions in the solution. A higher Na^+ concentration promotes the release of water from the geopolymer slurry, enhancing the interactions between water and other components. As a result, the friction and adhesion between the particles in the slurry are reduced, lowering the viscosity and improving the flowability of the slurry^[22].

As shown in **Figure 2**, the outflow time of the slurry under different dosages of sodium silicate exhibits a pattern of initially decreasing and then increasing. When the dosage of sodium silicate reaches a certain level, the concentration of sodium silicate in the geopolymer slurry becomes too high, which may lead to the formation of excessive gel-like or over-hydrated products between the sodium silicate and FBA geopolymer particles. These gel-like substances and hydrated products significantly increase the viscosity of the slurry, resulting in reduced flowability.

Moreover, excessive sodium silicate may also lead to the over-adsorption of free water in the system, causing the structure of the slurry to become more compact. This further restricts its flowability, leading to an increase in outflow time. Therefore, the change in flowability shows a trend of initially decreasing and then increasing, which is closely related to the gelation and accumulation of hydrated products caused by the excessive dosage of sodium silicate.

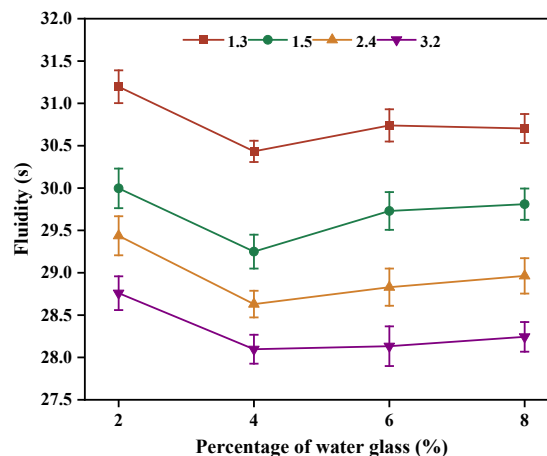


Figure 2. Influence of different sodium silicate modulus and dosage on slurry fluidity of geopolymer

3.2. Stability

The water separation rate of the geopolymer slurry under different sodium silicate moduli and dosages is shown in **Figure 3**. The stability of the geopolymer slurry changes with variations in the sodium silicate modulus and dosage. As illustrated in **Figure 3**, the water separation rate of the slurry with added sodium silicate is lower than that of the control group (12.05%), indicating an improvement in stability. The slurry's stability increases with a higher sodium silicate modulus. Specifically, within the modulus range of 1.5 to 2.4, the improvement in stability is more pronounced compared to the ranges of 1.3 to 1.5 and 2.4 to 3.2.

Under the same modulus, the water separation rate of the slurry first decreases and then increases as the sodium silicate dosage increases. For example, at a modulus of 1.5, as the dosage increases from 2% to 8%, the water separation rate of the slurry is 10.13%, 9.17%, 9.73%, and 9.88%, respectively. When the dosage exceeds 4%, the water separation rate rises significantly.

This behavior is due to the strong gelling properties of sodium silicate, which promote the formation of C-S-H or C-A-S-H gels in the geopolymer slurry. These hydration products help to form a more stable network structure, reducing the water separation rate and enhancing stability. However, excessive sodium silicate content may suppress the polymerization reaction, reducing the slurry's stability. Therefore, when preparing geopolymer grouting slurry, avoid excessive sodium silicate dosages that could adversely affect the slurry's stability^[23].

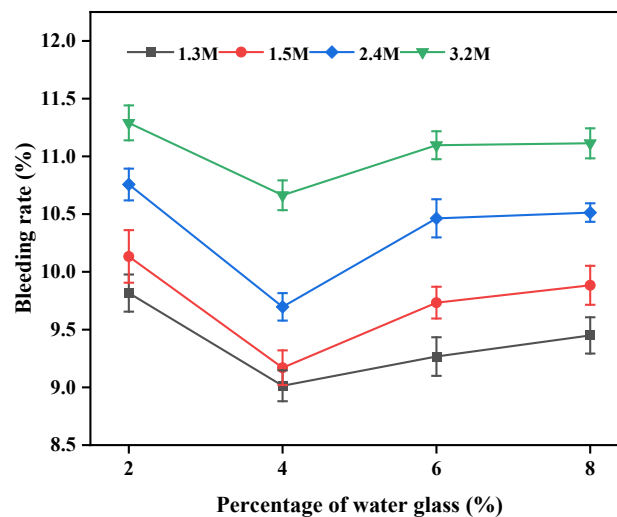


Figure 3. Influence of different sodium silicate modulus and dosage on the stability of geopolymer slurry

3.3. Compressive strength

The 28-day compressive strength of the geopolymer grouting material specimens with different sodium silicate moduli and dosages is shown in **Figure 4**. The compressive strength of the specimens at 28 days varies with different sodium silicate moduli and dosages. Under all sodium silicate moduli, the compressive strength of the geopolymer specimens is higher than that of the control group, which has a compressive strength of 3.27 MPa without sodium silicate. When the sodium silicate modulus is 1.3 and 1.5, the activation effect is more pronounced. At moduli of 2.4 and 3.2, the increase in compressive strength is relatively lower but still higher than that of the control group without sodium silicate.

At lower sodium silicate moduli, the concentration of silicate ions in the sodium silicate is higher, which can more effectively promote the reaction between the minerals in the mine tailings and the sodium silicate, generating more sulfoaluminate hydrate gels. This helps to enhance the compressive strength of the geopolymer. On the other hand, at higher moduli, the sodium silicate may produce fewer gels during hydration, leading to a less significant

improvement in compressive strength compared to lower moduli.

Under the same sodium silicate modulus, when the dosage exceeds 4%, the compressive strength of the geopolymer material starts to decline. This indicates that increasing the sodium silicate dosage can improve the compressive strength within a certain range. An appropriate amount of sodium silicate promotes the formation of more hydration products and enhances the network structure of the geopolymer. However, when the dosage is too high, it may lead to excessive hydration, causing an overly high concentration of sodium silicate in the system. This could negatively affect the reaction uniformity, resulting in the formation of excess hydration products and pores, which may reduce the compressive strength. Therefore, in practical applications, the sodium silicate dosage needs to be optimized to enhance the strength while avoiding excessive reactions.

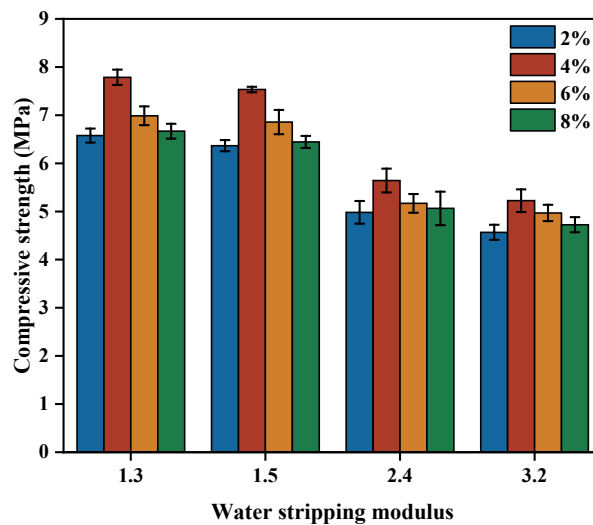


Figure 4. Influence of different sodium silicate modulus and dosage on 28 d compressive strength of geopolymer test block

In summary, the addition of water glass promotes the reaction between the mining waste and the components in the water glass, resulting in the formation of a denser hydration gel structure, thereby improving the stability and compressive strength of the furnace bottom ash geopolymer. The modulus and dosage of water glass are key factors influencing the enhancement of stability and strength. A moderate modulus and dosage can optimize the generation of hydration products, improving the stability and strength of the geopolymer material. Conversely, excessive dosage or an inappropriate modulus may lead to limited strength improvement or even a reduction in performance. Therefore, selecting the appropriate modulus and dosage of water glass is crucial to ensuring the performance of the geopolymer. Considering the flowability, stability, and compressive strength of the geopolymer grout material, as well as the economic cost, a water glass modulus of 1.5 and a dosage of 4% are determined for the furnace bottom ash geopolymer grout material.

3.4. Microscopic morphology

3.4.1. XRD analysis

XRD analysis was performed on geopolymer samples with the optimal water glass dosage and modulus, as well as representative samples without water glass after 28 d of curing (see **Figure 5**). The following conclusions can be drawn. After the optimal amount of water glass was added, the content of CaCO_3 , Al_2O_3 , and SiO_2 in the geopolymer decreased, while the C-A-S-H phase was generated. The XRD pattern indicates that the addition of water glass caused the dissolution of Al_2O_3 and SiO_2 in the alkaline environment, resulting in the formation of SiO_4^{4-} and AlO_4^{5-} ions. These ions are then combined with Ca^{2+} ions in the reaction system to form C-S-H and C-A-

S-H gels. These gel substances interconnect and bond, forming a denser mesh structure that effectively increases the cohesion between soil particles, significantly enhancing the strength of the sample. Therefore, under the optimal water glass dosage, the compressive strength of the geopolymer is significantly higher than that of the sample without water glass. This result indicates that the addition of water glass can improve the hydration reaction of the geopolymer, promote the formation of favorable gel phases, and thereby enhance its mechanical properties.

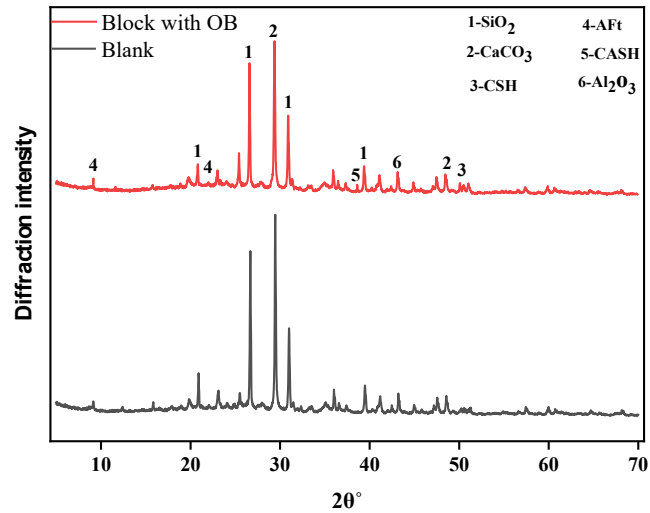


Figure 5. XRD spectra of optimum sodium silicate modulus and dosage and control group

3.4.2. SEM analysis

To investigate the effect of water glass on the internal microstructure of blast furnace slag-based geopolymer, SEM observations were conducted on samples cured for 28 d with and without water glass at the optimal dosage. Typical results are shown in **Figure 6**. As seen in **Figure 6**, it can be seen that the hydration products of the bottom ash geopolymer primarily consist of flaky and flocculent C-S-H gels, as well as needle-like ettringite. Compared to **Figure 6(a)**, the hydration products in **Figure 6(b)** have formed larger particle aggregates, which effectively fill the pores between the blast furnace slag and OB particles, as well as between particle clusters, forming a continuous structural network. This significantly improves the structure of the geopolymer, giving it a stacked and denser appearance^[24]. Such structural changes greatly enhance the compressive strength of the blast furnace slag-based geopolymer.

The above changes indicate that sodium silicate, as an effective admixture, plays an important role in promoting the hydration reaction, improving the morphology of hydration products, and enhancing the mechanical properties of FBA-based geopolymers, thereby proving its key role in the application of geopolymers.

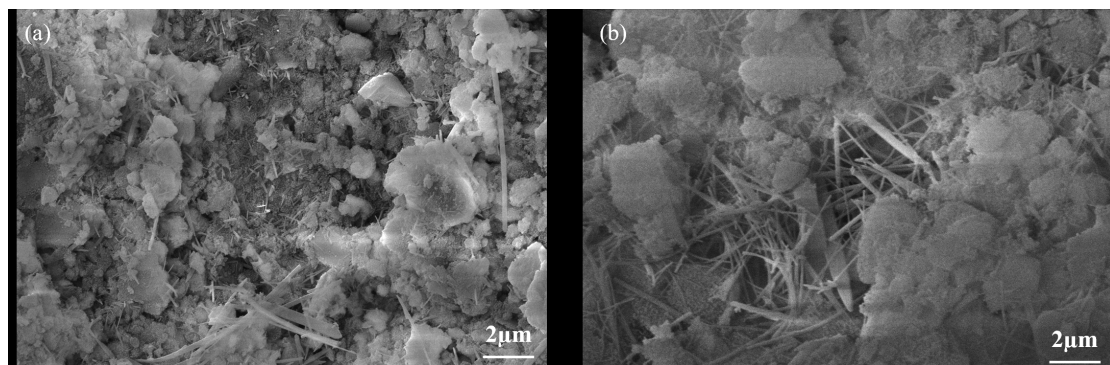


Figure 6. SEM comparison diagram: (a) control group, (b) optimal sodium silicate modulus and dosage

4. Crack diffusion simulation analysis

4.1. Governing equations

The diffusion of the slurry in the water-saturated fractures under dynamic water conditions conforms to the two-phase Darcy's law physical field in the Porous Media and Groundwater Flow module of COMSOL Multiphysics. Considering both water and slurry as incompressible, isotropic fluids, the generalized Darcy's law formula is as follows:

$$v = \frac{k}{\mu} \nabla p$$

$$v = s_o v$$

$$v = s_w v$$

$$s_o + s_w = 1$$

In the equations, s_o indicates the volume fraction of water within the fractures of the rock mass. The term v refers to the seepage velocity field, whereas v and v represent the flow rates of the slurry and water, respectively. The parameter μ is the viscosity of the slurry. Additionally, k signifies the permeability of the medium, and p is the pressure within the seepage field.

4.2. Fracture model

The three-dimensional single-fracture grouting model and the corresponding mesh division results are shown in **Figure 7**. It is assumed that the boundaries of the model are the rock mass boundaries, and the simulation considers only the slurry diffusion part. The fracture model is set to $2 \text{ m} \times 1 \text{ m} \times 2 \text{ m}$, the diameter of the grouting pipe is 0.053 m , and its length is 0.5 m . The left boundary of the model is the water inflow, the right boundary is the outflow, and the remaining boundaries are set to no flow.

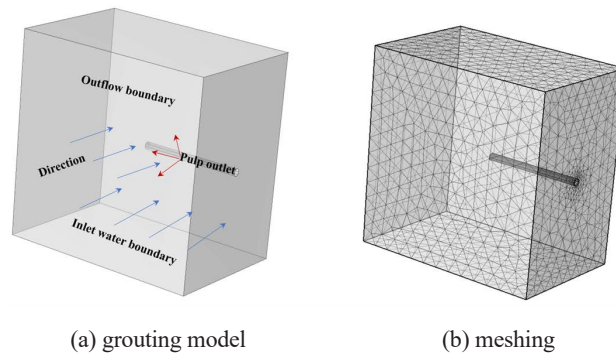


Figure 7. 3D single crack grouting model and mesh generation

To further investigate the performance of the furnace bottom ash geopolymers used as grouting materials, simulations were conducted using the research data of Zheng, which focused on ultra-fine cement slurry and slag-water glass as a control group for analysis^[25]. The specific properties of the slurry are provided in **Table 3**. The rock mass has a porosity of 0.35 and a permeability of $1 \times 10^{-12} \text{ m}^2$. The applied dynamic water pressure is 2 MPa , while the initial pressure for the grouting is also set to 2 MPa .

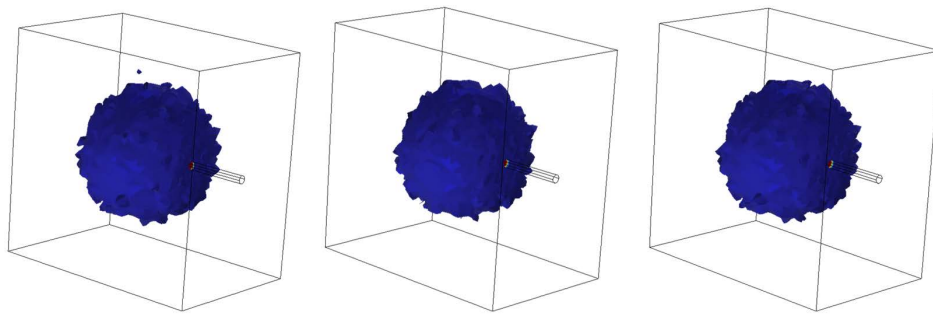
Table 3. Parameters related to numerical simulation

Fluids	Water	FBA solid waste slurry	Ultra-fine cement paste	Slag- water glass slurry
ρ ($\text{kg}\cdot\text{m}^{-3}$)	1,000	1,680	1,500	1,100
μ (Pa·s)	0.001	0.0378	0.012	0.003

4.3. Analysis of simulation results

4.3.1. Slurry volume fraction diffusion analysis

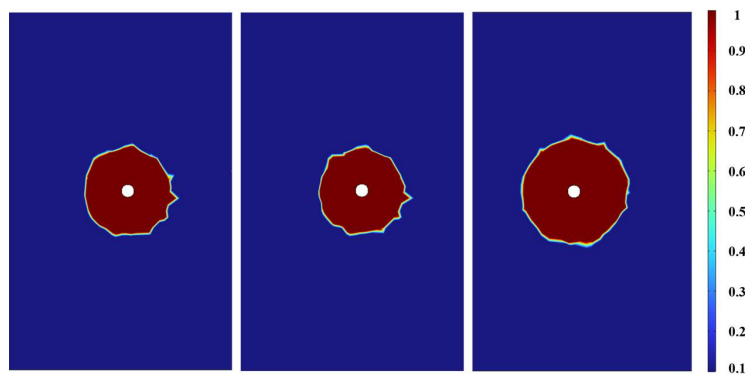
Taking a diffusion time of 5 seconds as an example, the volume fraction contour maps of different slurries are shown in **Figure 8**, and the volume fractions of the slurries at the same cross-section are shown in **Figure 9**. As seen in **Figure 9**, under dynamic water conditions, the volume fraction of the three slurries is significantly influenced by the direction of the water flow.



(a) superfine cement slurry (b) geopolymer slurry (c) slag-water glass slurry

Figure 8. Cloud image of volume fraction of different slurries

As shown in **Figure 9**, under dynamic water conditions, the slurry exhibits reverse diffusion, with the highest slurry concentration and volume fraction around the grouting pipe. The volume fraction and diffusion distance vary differently for each grouting material. Due to the higher density and viscosity of ultra-fine cement and geopolymer slurries compared to the slag-water glass slurry, the resistance during the diffusion process is greater, resulting in slower diffusion. Additionally, **Figure 8** and **Figure 9** show that the volume fraction and diffusion range of the geopolymer and ultra-fine cement slurries are similar, but the volume fraction of all three slurries does not increase with the expansion of the grouting diffusion range. This indicates that the viscosity of the slurry is non-linearly related to the grouting sealing effect, and the impact of dynamic water erosion on the grouting performance is significant.



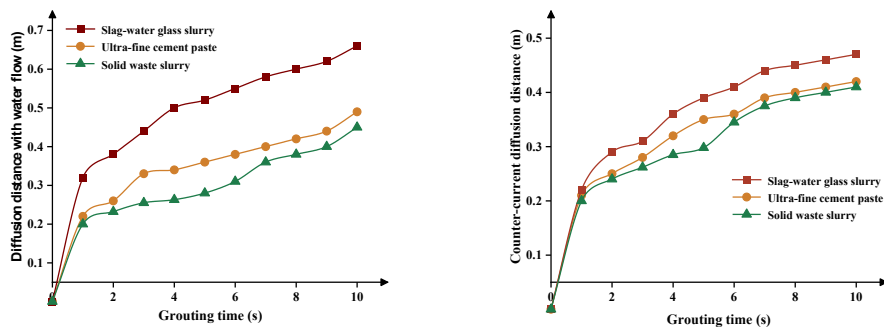
(a) Superfine cement slurry (b) terpolymer slurry (c) silica-sodium silicate slurry

Figure 9. Changes in volume fraction of different grout under dynamic water environment

4.3.2. Slurry diffusion distance analysis

Figure 10 displays the forward and reverse diffusion distances of various grouting materials in dynamic water circumstances. The viscosity of the slurry increases with time, and the reverse diffusion resistance progressively increases as well, stabilizing at a constant diffusion distance, as can be seen by comparing the diffusion distances of various slurries in the dynamic water environment depicted in Figure 10. Under the effect of water flow, the slag-water glass slurry has the lowest viscosity and the highest diffusion distance, the ultrafine cement slurry comes second, and the geopolymer slurry has the smallest diffusion distance. Subsequent investigation shows that the slurry's viscosity and diffusion distance have a negative correlation, confirming that all three slurries display specific regularities during reverse flow diffusion. Diffusion distance is greater in the slurry with lower viscosity and vice versa.

The maximum diffusion distances of the geopolymer and ultrafine cement slurries were compared, and it was discovered that there is an 8.16% difference in the forward diffusion distance and a 2.38% difference in the reverse diffusion distance. This finding implies that geopolymer slurry can partially substitute ultrafine cement grout components, lowering expenses without sacrificing grouting reinforcing efficacy.



(a) down-flow grout diffusion distance (b) down-flow grout diffusion distance

Figure 10. Different serious diffusion distances along and back

4.3.3. Analysis of the influence of grouting pressure on slurry diffusion distance

In dynamic water pressure environments, the diffusion distance of grouting materials is significantly influenced by grouting pressure. Taking geopolymer slurry as an example, different grouting pressures (2 MPa, 4 MPa, 6 MPa, 8 MPa, and 12 MPa) were applied for analysis to explore the reverse flow diffusion distance of the slurry under varying grouting pressures.

Using a diffusion time of 5 seconds as an example, the maximum reverse and forward diffusion distances under varying grouting pressures are shown in Figure 11. The diffusion behavior of geopolymer grouting materials at different grouting pressures is depicted in Figure 12. From Figure 11, it is clear that grouting pressure has a considerable effect on the diffusion extent of the slurry. Specifically, as the grouting pressure increases, there is a marked expansion in the diffusion range of the slurry.

As seen from Figure 11 and Figure 12, with the continuous increase in grouting pressure, the reverse diffusion distance of the slurry in the water flow gradually increases. This suggests that in actual grouting engineering applications, appropriately increasing the grouting pressure can effectively enhance the diffusion effect of the slurry, thereby improving the reinforcement effect of the grouting, especially in complex water environments.

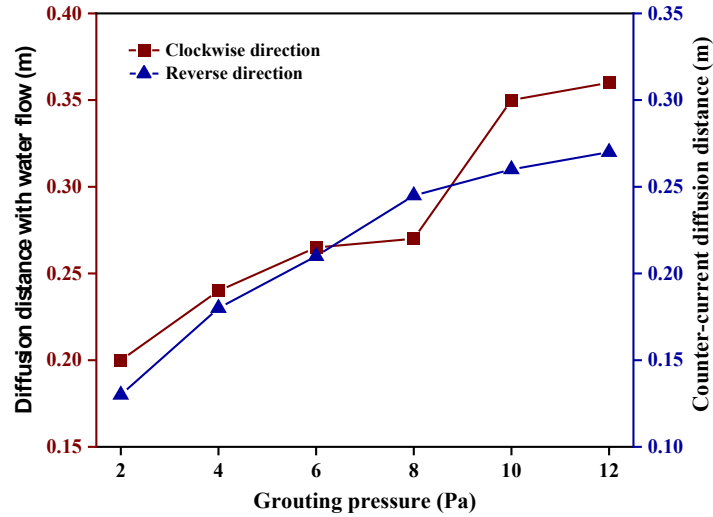


Figure 11. Diffusion distance of different mud in a dynamic water environment

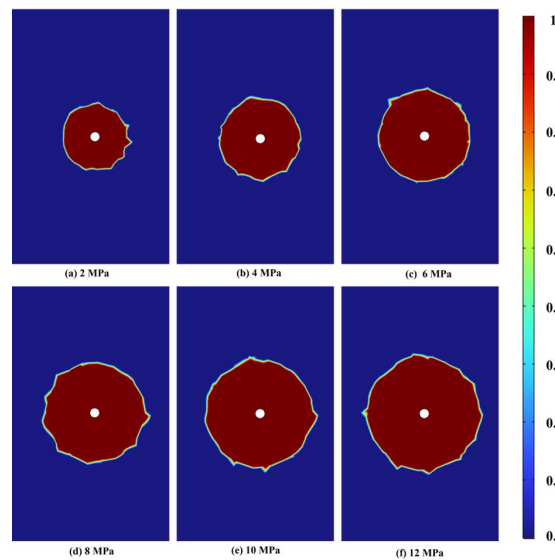


Figure 12. Diffusion law of polymer grouting materials under different grouting pressures

5. Conclusion

Based on the experimental results and numerical simulation analysis in this study, the following key conclusions are drawn.

- (1) Enhancement of geopolymer grouting material performance by sodium silicate: The addition of sodium silicate significantly improved the stability and compressive strength of the geopolymer grouting material. With a sodium silicate modulus of 1.5 and an addition rate of 4%, the stability of the slurry increased by 26.2%, and the 28-day compressive strength increased by 130.98%. As an important additive, sodium silicate enhances the gel structure of the geopolymer grout, thereby improving its stability and mechanical properties.
- (2) COMSOL numerical simulation analysis: The numerical simulation results indicate that the diffusion behavior of geopolymer slurry shows a trend similar to that of ultra-fine cement slurry. The slurry's resistance to scouring in dynamic water environments is closely related to its viscosity, with higher viscosity helping to improve the slurry's durability in cracks. Furthermore, appropriately increasing the

grouting pressure can promote the diffusion of the slurry in both downstream and upstream directions, improving its permeability and sealing effect.

- (3) Economic analysis: The production cost of geopolymers grouting materials is significantly lower than that of ultra-fine cement, demonstrating its significant economic advantage in practical applications. This cost advantage further confirms the superiority of geopolymers grouting materials in crack grouting and provides strong support for their wide application in fields such as water sealing in coal seam roofs and solid waste resource utilization.

Disclosure statement

The authors declare no conflict of interest

Funding

Enterprise entrusted funding Project (Project No. H23-467).

References

- [1] Tian S, Wang Y, Li H, et al., 2024, Analysis of the Causes and Safety Countermeasures of Coal Mine Accidents: A Case Study of Coal Mine Accidents in China from 2018 to 2022. *Process Safety and Environmental Protection*, 187: 864–875.
- [2] Lacoue-Labarthe T, Nunes PALD, Ziveri P, et al., 2016, Impacts of Ocean Acidification in a Warming Mediterranean Sea: An Overview. *Regional Studies in Marine Science*, 5: 1–11.
- [3] Han S, Chen H, Long R, et al., 2017, Evaluation of the Derivative Environment in Coal Mine Safety Production Systems: Case Study in China. *Journal of Cleaner Production*, 143: 377–387.
- [4] Yang R, Li Y, Guo D, et al., 2017, Failure Mechanism and Control Technology of Water-Immersed Roadway in High-Stress and Soft Rock in a Deep Mine. *International Journal of Mining Science and Technology*, 27(2): 245–252.
- [5] Yang W, He S, 2022, Coal Mine Safety Management Index System and Environmental Risk Model Based on Sustainable Operation. *Sustainable Energy Technologies and Assessments*, 53(C): 102721.
- [6] Liu Q, Dou F, Meng X, et al., 2021, Building Risk Precontrol Management Systems for Safety in China's Underground Coal Mines. *Resources Policy*, 74(C): 101631.
- [7] Li X, Zhang S, Ren R, et al., 2024, Comprehensive Evaluation and Spatial-Temporal Evolution Characteristics of Urban Resilience in Chengdu-Chongqing Economic Circle. *Chinese Journal of Population, Resources and Environment*, 22(1): 58–67.
- [8] Zhang J, Guan X, Li H, et al., 2017, Performance and Hydration Study of Ultra-Fine Sulfoaluminate Cement-Based Double Liquid Grouting Material. *Construction and Building Materials*, 132: 262–270.
- [9] Tang L, Wang Z, Zhang X, et al., 2023, Influence of Rheological Parameters on Cement Slurry Penetration Characteristics of Novel Oscillating Grouting Technology. *Construction and Building Materials*, 2023: 409.
- [10] Li Y, Chen M, Shi Q, et al., 2024, Biomass Fractionation Techniques Impact on the Structure and Antioxidant Properties of Isolated Lignins. *Separation and Purification Technology*, 330: 125499.
- [11] Wang J, Wang Y, Yu J, et al., 2022, Effects of Sodium Sulfate and Potassium Sulfate on the Properties of Calcium Sulfoaluminate (CSA) Cement Based Grouting Materials. *Construction and Building Materials*, 353: 129045.
- [12] Yang Y, Wang J, Dou H, 2014, Mechanical Properties of Anti-Seepage Grouting Materials for Heavy Metal Contaminated Soil. *Transactions of Nonferrous Metals Society of China*, 24(10): 3316–3323.

- [13] Wang M, Wang C, Yu J, et al., 2021, Investigation of the Grouting Effect of Blast Furnace Slag-Based Mortar on Void Road Bases Based on the Grouting Simulation Test. *Construction and Building Materials*, 282(4): 122567.
- [14] Li M, Bao S, Zhang Y, et al., 2024, Preparation and Characterization of Low-Activity Coal Bottom Ash-Based Cementitious Materials via Orthogonal Experiment. *Journal of Building Engineering*, 2024: 96.
- [15] Bakhrakh A, Solodov A, Naruts V, et al., 2017, High-Performance Self-Compacting Concrete with the Use of Coal Burning Waste. *IOP Conference Series: Earth and Environmental Science*, 90: 12213.
- [16] Pawluczuk E, Kalinowska-Wichrowska K, Jimenez JR, et al., 2021, Geopolymer Concrete with Treated Recycled Aggregates: Macro and Microstructural Behavior. *Journal of Building Engineering*, 2021: 44.
- [17] Fan G, Zhang D, Wang X, 2014, Reduction and Utilization of Coal Mine Waste Rock in China: A Case Study in Tiefa Coalfield. *Resources Conservation & Recycling*, 83: 24–33.
- [18] Yatsenko EA, Ryabova AV, Vil'bitskaya NA, et al., 2022, Eco-Geopolymers Based on CHP Plant Ash-Slag Waste: Promising Materials for Road Construction in the Arctic Zone. *Glass and Ceramics*, 78(11–12): 490–493.
- [19] Buch-Hansen M, 1997, Environment—A Liability and an Asset for Economic Development: Some Views on Environmental Protection with Economic Development in Bhutan. *International Journal of Sustainable Development & World Ecology*, 4: 17–27.
- [20] Buchdahl JM, Raper D, 2015, Environmental Ethics and Sustainable Development. *Sustainable Development*, 2015: 6.
- [21] Ren C, Li KQ, Wang Y, et al., 2023, Preparation and Hydration Mechanisms of Low Carbon Ferrochrome Slag-Granulated Blast Furnace Slag Composite Cementitious Materials. *Materials*, 2023: 16.
- [22] Rao AP, Rao AV, Pajonk GM, 2007, Hydrophobic and Physical Properties of the Ambient Pressure Dried Silica Aerogels with Sodium Silicate Precursor Using Various Surface Modification Agents. *Applied Surface Science*, 253(14): 6032–6040.
- [23] Bilondi MP, Toufigh MM, Toufigh V, 2018, Experimental Investigation of Using a Recycled Glass Powder-Based Geopolymer to Improve the Mechanical Behavior of Clay Soils. *Construction and Building Materials*, 170: 302–313.
- [24] Wang C, Zhao L, Guo Z, et al., 2024, Mechanistic Study of Fly Ash Activity Enhanced by High Temperature to Strengthen Cementitious Materials. *Construction and Building Materials*, 2024: 416.
- [25] Dong-Zhu Z, Qing-Song Z, Peng LI, et al., 2017, Numerical Simulation of Dynamic Grouting in Drift Sand Strata. *Computer Simulation*, 34(1): 241–244 + 309.

Publisher's note

Bio-Byword Scientific Publishing remains neutral with regard to jurisdictional claims in published maps and institutional affiliations.